SPIN
Vol. 3, No. 3 (2013) 1340001 (7 pages)

DOI: 10.1142/S2010324713400018

World Scientific
www.worldscientific.com

ROLLED-UP PERMALLOY NANOMEMBRANES WITH MULTIPLE WINDINGS

ROBERT STREUBEL
Institute for Integrative Nanosciences
IFW Dresden, 01069 Dresden, Germany

Material Systems for Nanoelectronics
Chemnitz University of Technology, 09107 Chemnitz, Germany
r.streubel@ifw-dresden.de

DENYS MAKAROV
Institute for Integrative Nanosciences
IFW Dresden, 01069 Dresden, Germany
d.makarov@ifw-dresden.de

JEHYUN LEE
Department of Materials Science and Engineering
National Creative Research Center for Spin Dynamics &
Spin-Wave Devices, and Nanospinics Laboratory
Seoul 151-744, Republic of Korea

Research Institute of Advanced Materials
Seoul National University, Seoul 151-744, Republic of Korea
jehyun.lee@gmail.com

CHRISTIAN MÜLLER
Measurement and Sensor Technology
Chemnitz University of Technology, 09107 Chemnitz, Germany
christian.mueller@etit.tu-chemnitz.de

MICHAEL MELZER
Institute for Integrative Nanosciences
IFW Dresden, 01069 Dresden, Germany
m.melzer@ifw-dresden.de

RUDOLF SCHÄFER
Institute for Metallic Materials
IFW Dresden, 01069 Dresden, Germany

Institute for Materials Science, Dresden University of Technology
01069 Dresden, Germany
r.schaefer@ifw-dresden.de

CARLOS CESAR BOF BUFON
Institute for Integrative Nanosciences, IFW Dresden
01069 Dresden, Germany

Brazilian Nanotechnology National Laboratory
CNPEM, PO Box 619, 13083-970, Campinas, SP, Brazil
cesar.bof@lnnano.org.br

SANG-KOOG KIM
Department of Materials Science and Engineering
National Creative Research Center for Spin Dynamics &
Spin-Wave Devices, and Nanospinics Laboratory
Seoul 151-744, Republic of Korea

Research Institute of Advanced Materials, Seoul National University
Seoul 151-744, Republic of Korea
sangkoog@snu.ac.kr

OLIVER G. SCHMIDT
Institute for Integrative Nanosciences
IFW Dresden, 01069 Dresden, Germany

Material Systems for Nanoelectronics
Chemnitz University of Technology, 09107 Chemnitz, Germany

Merge Technologies for Multifunctional Lightweight Structures
Chemnitz University of Technology, 09107 Chemnitz, Germany
o.schmidt@ifw-dresden.de

Received 12 April 2013
Accepted 6 August 2013
Published 18 October 2013

We fabricated Permalloy ($Fe_{19}Ni_{81}$) nanomembranes rolled-up into compact three-dimensional architectures and experimentally investigated their magnetic and magneto-electric responses. When a magnetic nanomembrane is rolled-up, an additional magnetostatic interaction between the multiple windings emerges. Such kind of magnetostatic interaction, unique to the rolled-up magnetic nanomembranes and not accessible in any other magnetic architecture, is addressed for the first time in this study. An important feature of rolled-up tubes with multiple windings is that the inner and outer windings are formed by a single magnetic sheet; the spin configuration therefore must be continuous. The magnetostatic interaction induces anti-parallel alignment of the spins within adjacent layers of a rolled-up nanomembrane. The interplay between the magnetostatic interaction due to geometrical transformation and the exchange coupling in the film results in a stabilization of stripe domain patterns.

Keywords: Rolled-up nanotechnology; magnetic nanomembranes; magnetic tubes; micromagnetic calculations; anisotropic magnetoresistance.

1. Introduction

The impressive success of nano-/micro-electro-mechanical systems (NEMS/MEMS) has been driven by the development and implementation of novel architectures with advanced functionalities. These new building blocks promise to fulfill the requirements of miniaturization, which are typically realized by extensively shrinking the elements

laterally. As this strategy busts up against physical limits, there are intensive ongoing efforts to find novel technological approaches. For instance, going beyond planar two-dimensional solutions by exploring the third dimension is a breakthrough in the engineering of multifunctional compact architectures for on-chip applications.[1,2] The crucial aspect of this technology is the exploitation of flexible ultra-thin membranes in multifunctional devices directly on-chip integrable by currently available main-stream technologies.

In the last decade, rolled-up nanotechnology was introduced that relies on the release of a strained nanomembrane from a sacrificial layer, leading to bending of the nanomembrane and resultant transformation into a tube of predetermined size and geometry.[3–5] Great advances in the creation of rolled-up architectures have already been shown by implementing optical[6,7] and electronic elements[8,9]; Catalytic rolled-up tubes as required for chemical and biological applications were already developed.[10,11] In the family of rolled-up functional elements, rolled-up magnetic nanomembranes[5,12,13] have yet to reach their full application potential.[14,15] This is mainly due to difficulties in understanding and predicting integral magnetic or magneto-electric responses of such complex three-dimensional architectures.[16] In this respect, static and dynamic characteristics of magnetic structures to an external magnetic field, such as hysteresis loop and high-frequency alternating field, are strongly influenced by their spin configurations.[17–20]

One of the most striking features of rolled-up magnetic nanomembranes with multiple windings is the emergent magnetostatic interaction between adjacent windings. As the inner and outer windings are formed by a single magnetic nanomembrane, the spin configuration throughout the entire structure has to be continuous, and spins cannot be separated. Accordingly, the magnetic pattern of a rolled-up tube is expected to be more complicated than that of a closed one, which are typically produced by electrochemical depositions onto nanoholes or nanorods,[23] are apt to have a closed loop of spins in the azimuthal direction.[21,22] These closed tubes reduce the magnetostatic energy by circulating the spins around the tube axis under proper geometrical conditions.[24]

In the present study, we fabricated Permalloy ($Fe_{19}Ni_{81}$) nanomembranes rolled-up into a compact three-dimensional architecture and experimentally investigated their magnetic and magneto-electric responses. By measuring individual rolled-up tubes, we are able to access key parameters of magnetic hysteresis loops (remanence, coercivity) as well as to visualize the complex remanent magnetic domain pattern by means of Kerr microscopy.

2. Sample Preparation

Layers consisting of strained $SiO(10)/SiO_2(40)$ covered by $Pt(2)/Py(20)/Pt(2)/Al_2O_3(4)$ (thickness given in nanometers) were grown onto $Si(100)/SiO_x(1\,\mu m)$ substrates with a 20 nm-thick GeO_x buffer layer. A schematic of the sample fabrication process is provided in Fig. 1(a). In brief, an initial GeO_x sacrificial layer was prepared by sputtering. Then, a strained bi-layer consisting of SiO and SiO_2 was deposited onto the sacrificial layer by electron beam evaporation at deposition rates of 5 Å/s and 0.5 Å/s, respectively. Afterwards, a Pt/Py/Pt trilayer was deposited by room-temperature magnetron sputtering at deposition rates of 0.7 Å/s and 0.55 Å/s for Pt and Py, respectively. Subsequently, the samples were transferred to an atomic layer deposition (ALD) chamber and covered with a 4 nm-thick Al_2O_3 layer. The electrical contact pads made of Cr(10)/Au(50) were prepared by electron beam evaporation. Finally, the samples were patterned by standard photolithography; the pattern size was chosen such that tubes with about 1 and 2 windings were formed. In order to define the rolling direction, a trench was opened at one side of the planar structure by first etching the Al_2O_3 in 3% hydrogen fluoride solution, followed by partial etching of the GeO_x layer in H_2O_2 (30%). The releasing of the nanomembrane from the host substrate was initiated by immersing the structure in H_2O_2 (0.03%) solution at 50°C. After 4 h, the samples were transferred into pure deionized water and kept at room temperature for two days to complete the rolling process. Finally, the samples were immersed in 50°C water for 2 h in order to remove the remaining content of GeO_x. Figure 1(b) shows a scanning electron micrograph of the rolled-up nanomembrane (initial, pre-roll-up size of rectangle: $250 \times 45\,\mu m$). The depicted tube, consisting of about 1.2 windings, has a diameter of $(11.2 \pm 0.5)\,\mu m$. Its cross-section is shown in the inset. The rolling direction and contact pads are sketched in the image.

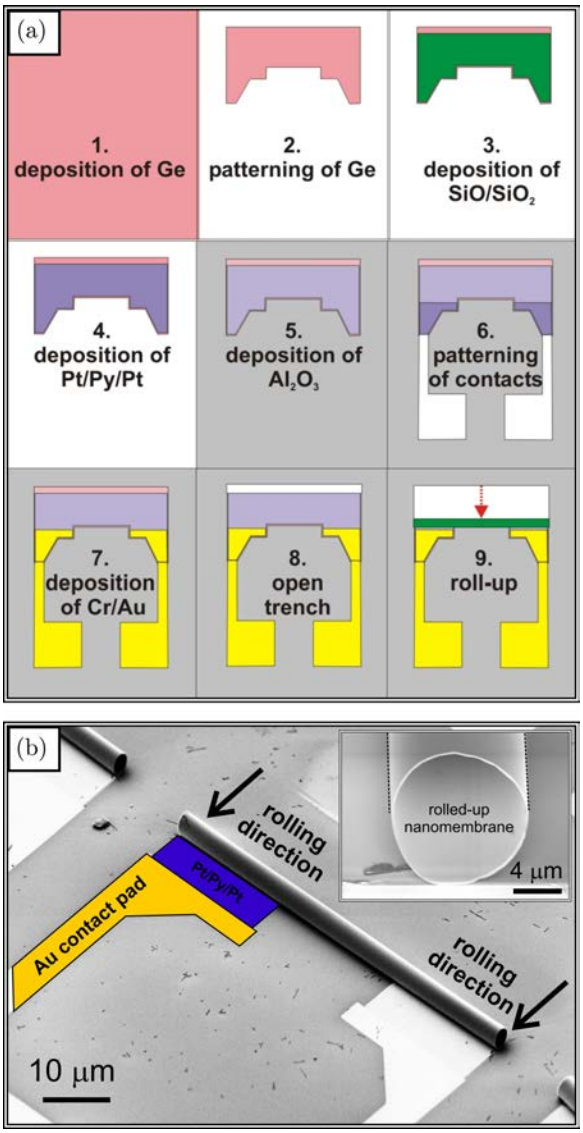

Fig. 1. (a) Schematics of the fabrication of rolled-up Py nanomembranes. (b) Scanning electron micrograph of a rolled-up Py tube connected to electric contacts. The inset shows the cross-section of the (11.2 ± 0.5) μm diameter tube, which consists of about 1.2 windings.

3. Results and Discussion

The magnetization reversals of single rolled-up tubes with 1.2 and 2.5 windings were experimentally measured by means of longitudinal magneto-optical Kerr effect (MOKE) magnetometry (Fig. 2). This method is sensitive to the in-plane magnetization component and reveals the (anti-)parallel components with respect to the external magnetic field. All measurements were carried out at room temperature with a field sweep rate of 3 Hz up to 100 Oe strength. The spot size of the laser beam was about 10 μm, which is suitable to investigate individual rolled-up tubes. Due to strong scattering from a tubes curved surface, the magnetic hysteresis loop was averaged over 5000 cycles to achieve a moderate signal-to-noise ratio for the rolled-up nanomembranes with 1.2 windings (Fig. 2(a)). The values of the coercive and saturation fields measured with the magnetic fields applied along the tube axis (0°) are (2.0 ± 0.5) Oe and (12 ± 2) Oe, respectively. When the magnetic field is aligned perpendicular to the tube axis (90°), the values of the coercive and saturation fields increase to (7.0 ± 0.5) Oe and (15 ± 2) Oe, respectively. These are significantly larger than those measured for planar sheets prior to rolling (Fig. 2(a), solid lines). It is important to note that the planar reference sample had a small in-plane shape anisotropy with an axis perpendicular to the rolling direction. However, after the rolling process, the sample does not reveal full remanence neither for transverse nor longitudinal orientation: the remanent magnetization normalized by the saturation magnetization is about 0.5 (0.2) when the field was applied along (perpendicular to) the tube axis. This suggests that the long axis of the tube is not the easy axis of magnetization, and hints at a complex magnetic domain pattern.

This assumption is verified by Kerr microscopy of magnetic domains on tubular architectures (Figs. 2(b) and 2(c)). Please note that due to the curvature, only a narrow stripe on top of the tube can be focused during imaging. The remanent states after ac-field demagnetization along and perpendicular to the tube axis are shown in Fig. 2(b). Based on the Kerr contrast, we conclude that both magnetization and magnetic domain walls form a spiral. It is important to mention that the experimentally observed domain patterns are still 2D images. However, the investigated objects are true 3 dimensional and an interpretation of the obtained Kerr microscopy data is not straightforward. To interpret the experimental finding, micromagnetic simulations will need to be carried out. Therefore, in the present work, assignment of the magnetic domain pattern to form a spiral is based on pure geometrical consideration taking into account the symmetry of the object. Figure 2(c) shows a series of magnetization distribution snapshots by Kerr microscopy during the magnetization reversal in a magnetic field applied perpendicular to the tube axis. Starting from saturation, the tube is magnetized perpendicular to its main axis (except a pinning side). With decreasing

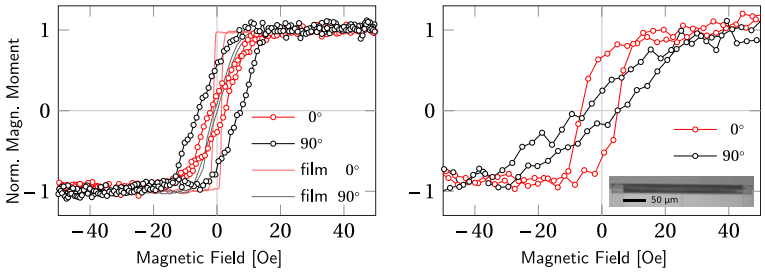

(a) Tube with 1.2 windings (d) Tube with 2.5 windings

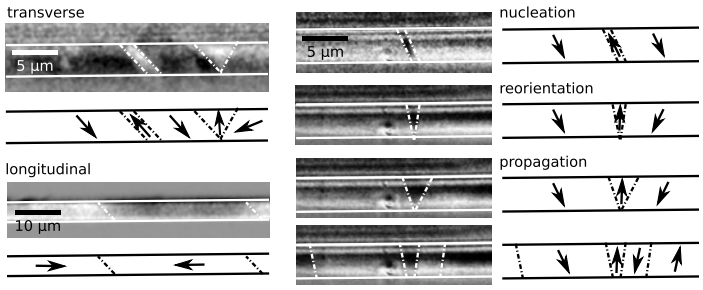

(b) Remanent states (c) Magnetization reversal–perp. to tube axis

Fig. 2. Hysteresis loops of a rolled-up Py tube with (a) 1.2 windings and 11 μm diameter and (d) 2.5 windings and 19 μm diameter. An external magnetic field is applied along the tube axis (0°) and perpendicular to it (90°). Measurement of the sample before rolling (planar layout) is shown in dashed lines in (a). Kerr microscopy data from the sample with 1.2 windings is shown in (b) and (c). (b) Remanent magnetic states after ac demagnetization with magnetic field applied perpendicular to (top panel) and along the tube axis (bottom panel). (c) Snapshots reveal the evolution (images from top to bottom) of magnetic pattern during magnetization reversal process in a magnetic field applied perpendicular to the tube axis. Schematics of the magnetic pattern are given under/next to each Kerr micrograph.

magnetic field, the magnetic domains of opposite orientation expand from the bottom to the top side of the tube. These domains are separated by slightly tilted domain walls similar to those observed in the remanent state.

In analogy to the discussion above, magnetization reversal of rolled-up nanomembranes with 2.5 windings occurs via nucleation of magnetic domain walls and their propagation along the tube (Fig. 2(d)). Magnetic domain walls are tilted at an angle comparable to the sample with 1.2 windings. However, the magnetic hysteresis loops measured for the rolled-up tubes with 1.2 and 2.5 windings are qualitatively different. The shape anisotropy of the sample increases with larger number of windings. As the samples contain a nonmagnetic spacer between the windings, the increase of the shape anisotropy is assigned to be driven by magnetostatic coupling between the windings.

The peculiar magnetic domain pattern observed in the rolled-up Py nanomembranes is expected to have an impact on their magneto-electric properties. For confirmation, we measured the anisotropic magnetoresistive (AMR) response of the rolled-up samples with 1.2 windings and compare it to the unrolled planar reference sample to identify the special magnetoresistive features induced by the geometrical transformation. The samples are mounted onto a chip carrier, and the individual structures are contacted using wedge bonding to inject a probe current along the tube axis. For the characterization, the chip carrier is positioned between the pole shoes of an electromagnet (maximum field applied: ± 500 Oe) at different in-plane angles relative to the direction of the applied magnetic field, and AMR curves are recorded for each angle. The AMR is defined as the ratio of the maximum resistance change to the minimum resistance. Figure 3(a) shows the angular dependence of the AMR magnitude for the rolled-up and planar Py nanomembranes. The solid lines refer to the uncertainty. The planar sample exhibits a large AMR ratio when applying the field along the short axis of the planar membrane (Fig. 3(b)), since the magnetization aligns perpendicular to the electrical current at saturation (Fig. 3(a), red curve with

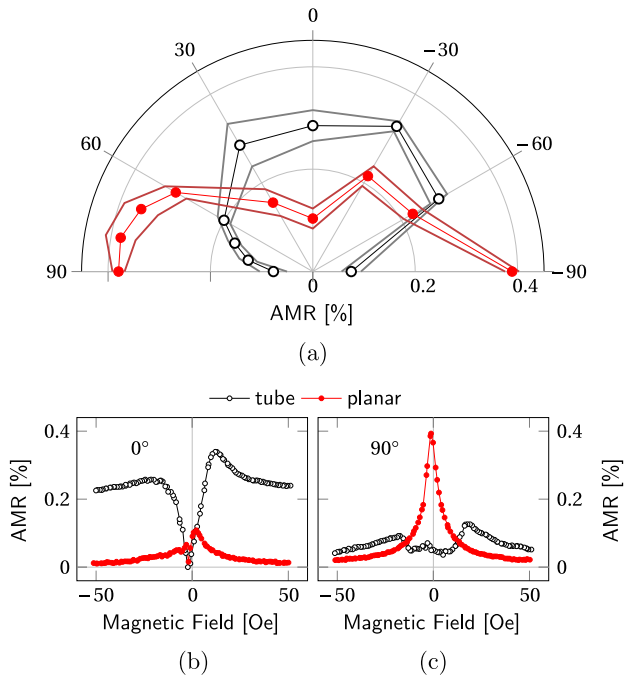

Fig. 3. AMR data obtained for rolled-up tube (open symbols) and planar sample before rolling (closed symbols). (a) Angular dependence of AMR in both samples. The solid lines refer to the uncertainty. The AMR as a function of the fields was applied (b) along (0°) and (c) perpendicular (90°) to the tube axis.

symbols). In contrast to this magnetization rotation process, the magnetization reversal for longitudinally applied magnetic field is governed by the nucleation of magnetic domains with reversed orientation, which causes a small overall AMR signal (Fig. 3(c)). Individual AMR curves of the rolled-up and planar nanomembranes in the magnetic field applied along or perpendicular to the tube axis are presented in Figs. 3(b) and 3(c), respectively.

For the rolled-up nanomembranes, the angular dependence and AMR curves of the rolled-up nanomembranes differ substantially from the planar case. While planar structures exhibit an AMR minimum along the current direction (0°), the tubular architecture shows a maximum (Fig. 3(a)). It should be noted that recently, Rüffer *et al.*[24] performed first experimental studies on transport in individual tubular structures with 150 nm diameter prepared using the anodization approach. Even for these rather small tubular architectures, the authors had to consider six distinct magnetic states to explain their experimental findings.[24] The distinct feature of the present study about rolled-up magnetic nanomembranes is their spiral-like geometry, which includes a nanomagnetic spacer between windings and a larger diameter, resulting in an increase of both the number of possible magnetic states and of their complexity.

Based on a combined analysis of AMR and MOKE data, a possible explanation for the magneto-electric behavior of the rolled-up Py nanomembranes is as follow. When the magnetic field is applied along the tube axis, the spins align at saturation in the same direction. As the electrical current flows in this direction, a high resistance is detected. At remanence the spins align azimuthally and thus perpendicular to the current, decreasing the resistance substantially toward smaller fields. When the field is applied perpendicularly to the tube axis, a complex domain pattern develops during the magnetization reversal process, as revealed by Kerr microscopy (Fig. 2(d)). Since the magnetization points preferentially in the azimuthal direction, the major portion of the magnetic moments is aligned perpendicularly to the current, resulting in a small AMR ratio. Note that the experimental curve drawn for the rolled-up nanomembrane at 0° has an additional maximum at a field of about 15 Oe. This feature is related to the chosen contact geometry wherein the electrical current flows through planar segments of the Pt/Py/Pt trilayer before and after the tubular architecture (Fig. 1(b)). In these areas, the current is perpendicular to the field direction.

4. Conclusion

We investigated the influence of the rolled-up geometry on magnetic characteristics of curved magnetic nanomembranes. The results revealed the dominant influence of the magnetostatic interaction between multiple windings of rolled-up nanomembranes inducing anti-parallel alignment of the moments between adjacent layers of the rolled-up tube. This leads to the stabilization of complex spiral-like magnetic domains in tubular architectures. The impact of the peculiar magnetic domain pattern observed in the rolled-up Py nanomembranes on magneto-electric properties is addressed as well.

Acknowledgments

The authors thank C. Krien, M. E. Navarro-Fuentes and C. Vervacke, B. Eichler (IFW Dresden) for their help in sample fabrication. This work was supported by the Basic Science Research Program through the National Research Foundation of Korea (NRF)

funded by the Ministry of Education, Science and Technology (No. 20120000236) and by the German Science Foundation (DFG) grants MA 5144/2-1, MU2766/3-1, DFG Research Unit 1713 and the European Research Council under the European Union's Seventh Framework Programme (FP7/ 2007-2013)/ERC grant agreement No. 306277.

References

1. J. A. Rogers, M. G. Lagally and R. G. Nuzzo, *Nature* **477**, 45 (2011).
2. O. G. Schmidt, N. Schmarje, C. Deneke, C. Müller and N.-Y. Jin-Phillipp, *Adv. Mater.* **13**, 756 (2001).
3. V. Y. Prinz, V. A. Seleznev, A. K. Gutakovsky, A. V. Chehovskiy, V. V. Preobrazhenskii, M. A. Putyato and T. A. Gavrilova, *Physica E: Low-Dimens. Syst. Nanostruct.* **6**, 828 (2000).
4. O. G. Schmidt and K. Eberl, *Nature* **410**, 168 (2001).
5. Y. Mei, G. Huang, A. A. Solovev, E. Bermúdez Ureña, I. Mönch, F. Ding, T. Reindl, R. K. Y. Fu, P. K. Chu and O. G. Schmidt, *Adv. Mater.* **20**, 4085 (2008).
6. T. Kipp, H. Welsch, Ch. Strelow, Ch. Heyn and D. Heitmann, *Phys. Rev. Lett.* **96**, 077403 (2006).
7. S. Mendach, R. Songmuang, S. Kiravittaya, A. Rastelli, M. Benyoucef and O. G. Schmidt, *Appl. Phys. Lett.* **88**, 111120 (2006).
8. E. J. Smith, W. Xi, D. Makarov, I. Mönch, S. Harazim, V. A. Bolanos Quinones, C. K. Schmidt, Y. Mei, S. Sanchez and O. G. Schmidt, *Lab Chip* **12**, 1917 (2012).
9. D. Grimm, C. C. Bof Bufon, C. Deneke, P. Atkinson, D. J. Thurmer, F. Schäffel, S. Gorantla, A. Bachmatiuk and O. G. Schmidt, *Nano Lett.* **13**, 213 (2013).
10. A. A. Solovev, Y. Mei, E. Bermúdez Ureña, G. Huang and O. G. Schmidt, *Small* **5**, 1688 (2009).
11. S. Sanchez, A. A. Solovev, Y. Mei and O. G. Schmidt, *J. Am. Chem. Soc.* **132**, 13144 (2010).
12. F. Balhorn, S. Mansfeld, A. Krohn, J. Topp, W. Hansen, D. Heitmann and S. Mendach, *Phys. Rev. Lett.* **104**, 037205 (2010).
13. E. J. Smith, D. Makarov, S. Sanchez, V. M. Fomin and O. G. Schmidt, *Phys. Rev. Lett.* **107**, 097204 (2011).
14. E. Bermúdez Ureña, Y. Mei, E. Coric, D. Makarov, M. Albrecht and O. G. Schmidt, *J. Phys. D: Appl. Phys.* **42**, 055001 (2009).
15. I. Mönch, D. Makarov, R. Koseva, L. Baraban, D. Karnaushenko, C. Kaiser, K.-F. Arndt and O. G. Schmidt, *ACS Nano* **5**, 7436 (2011).
16. C. Müller, C. C. Bof Bufon, M. E. Navarro Fuentes, D. Makarov, D. H. Mosca and O. G. Schmidt, *Appl. Phys. Lett.* **100**, 022409-4 (2012).
17. I. Betancourt, G. Hrkac and T. Schrefl, *J. Appl. Phys.* **104**, 023915-6 (2008).
18. M. Yan, C. Andreas, A. Kakay, F. Garcia-Sanchez and R. Hertel, *Appl. Phys. Lett.* **99**, 122505-3 (2011).
19. R. Streubel, D. J. Thurmer, D. Makarov, F. Kronast, T. Kosub, V. Kravchuk, D. D. Sheka, Y. Gaididei, R. Schäfer and O. G. Schmidt, *Nano Lett.* **12**, 3961 (2012).
20. J. A. Otalora, J. A. Lopez-Lopez, P. Vargas and P. Landeros, *Appl. Phys. Lett.* **100**, 072407 (2012).
21. D. Rüffer, R. Huber, P. Berberich, S. Albert, E. Russo-Averchi, M. Heiss, J. Arbiol, A. Fontcuberta i Morral and D. Grundler, *Nanoscale* **4**, 4989 (2012).
22. D. P. Weber, D. Rüffer, A. Buchter, F. Xue, E. Russo-Averchi, R. Huber, P. Berberich, J. Arbiol, A. Fontcuberta i Morral, D. Grundler and M. Poggio, *Nano Lett.* **12**, 6139 (2012).
23. K. Nielsch, F. J. Castaño, S. Matthias, W. Lee and C. A. Ross, *Adv. Eng. Mater.* **7**, 217 (2005).
24. X. F. Han, S. Shamaila, R. Sharif, J. Y. Chen, H. R. Liu and D. P. Liu, *Adv. Mater.* **21**, 4619 (2009).